PUNE RESEARCH TIMES ISSN 2456-0960
AN INTERNATIONAL JOURNAL OF CONTEMPORARY STUDIES VOL 2, ISSUE 2

OSCILLATORY FREE CONVECTIVE HEAT TRANSFER THROUGH A POROUS MEDIUM IN A VERTICAL WAVY CHANNEL WITH QUADRATIC TEMPERATURE VARIABLE

DR. K. GNANESWAR
Principal,
S.K.P. Government Degree College,
Guntakal, Anantapuramu-Dist,
(AP) INDIA.

ABSTRACT

In this chapter we have investigated unsteady oscillatory free convective heat transfer through a viscous fluid is a porous medium confined in a vertical wavy channel with quadratic density temperature variable. The unsteadiness in the flow is due to an oscillatory flux in the fluid region with quadratic density-temperature variation. The equations governing the flow and heat transfer have been solved by perturbation technique with δ, the slope of the wavy walls as a perturbation parameters. The velocity and the temperature have been analyzed for different variations of the governing parameters G, R, D^{-1},α, β, x and t. Also the stress and rate of heat transfer are evaluated numerically for different variations of the parameters.

Keywords : *Porous medium; Vertical wavy channel; Quadratic temperature variable; Oscillatory flux; Perturbation technique.*

I NTRODUCTION

Unsteady convection flows play an important role in aerospace technology, turbo machinery and chemical Engineering. Such flows arise due to either unsteady motion of a boundary or boundary temperature. Unsteadiness may also be due to oscillatory free stream velocity or temperature. These oscillatory free convective flows are important from technological point of view. Nanda and Sharma (12) have discussed the unsteady free convective flow past a semi-finite plate with oscillatory wall temperature and shown the existence of similarity solution. Later Soundalgekar and Pop (18) have solved this problem using momentum – integral method. Kellecher and Yang (22) have studied different aspect of this problem.

In recent years, energy and material saving considerations have prompted an expansion of the efforts at producing efficient heat exchange equipment through augmentation of the heat transfer. The heat transfer through wavy channel has been a topic of interest in recent times owing to its applications in technological areas viz., transpiration cooling of re-entry vehicles and rocket boosters, cross-hatching of an ablative surface and film vaporization in combustion chambers. It has been established (15) that channels with diverging-converging geometries augment the transportation of heat transfer and momentum. As the fluid flows through a tortuous path viz., the dilated –constricted geometry, there will be more intimate contact between them. The flow takes place both axially (primary) and transversely (secondary) with the secondary velocity being towards the axis in the fluid bulk rather than confining with in a thin layer as in straight channels. Hence it is advantageous to go for diverging –converging geometries for improving the design of heat transfer equipment.

Puroshotham Reddy (14) has investigated oscillatory convective heat transfer in a vertical wavy channel. Sree Ramachandra Murthy (19) has investigated the unsteady mixed convective heat transfer through a porous medium in a vertical wavy channel with oscillatory flux. Recently Ravindra Nath (17) has investigated oscillatory convective heat transfer through a porous medium in a horizontal wavy channel. Gayathri (8) has analyzed the effect of radiation on the free convective heat transfer flow in a horizontal wavy channel. Bharathi (4) has discussed radiation effect on oscillatory convective flow through a porous medium in a vertical channel bounded by flat walls. In all the above investigations the density variation is taken linearly, but there are some circumstances where the density variation is non-linear.

Radiative flow plays a vital role in many industrial and environmental process, example, heating and cooling chambers, fossil fuel combustion energy process, evaporation from large open water reservoirs, astro physical flows, solar power technology and space vertical-re-entry. Taneja ET. al., (20) have studied the effect of magnetic field on free convective flow through porous medium with radiation and variable permeability in the slip flow regime. Kumar Atul (10) studied the effect of magneto hydro dynamics free convection flow of viscous fluid past a porous vertical plate through non-homogeneous porous medium with radiation and temperature gradient dependent heat source in slip flow regime. The effect of convection flow with thermal radiation and mass transfer past a moving vertical porous plate was studied by Makinde (11). Ayani (2) studied the effect of radiation on the laminar natural convection induced by a line source. Raptis (16) have discussed the effect of radiation and free convection flow through porous medium. Magneto hydrodynamics oscillatory flux on free convection radiation through a porous medium with constant suction velocity was investigated by El. Hakeem (5). Alagoa et. al., (1) studied radiative and free convection effects on MHD flow through porous medium between infinite parallel plates with time dependent suction. Bestman and Adjepong (3) analyzed unsteady hydro magnetic free convection flow with radiative heat transfer in a rotating fluid. Free convection flow has attracted by attention of many research workers due to dissipation is generally neglected. The

radiation effect on unsteady convective heat transfer has been analyzed by Ramana (15) and Jaffarunnisa (9) in vertical channels under different condition.

In this chapter we investigate the unsteady oscillatory free convective heat transfer through a viscous fluid is a porous medium confined in a vertical wavy channel with quadratic density temperature variable. The unsteadiness in the flow is due to an oscillatory flux in the fluid region with quadratic density-temperature variation. The equations governing the flow and heat transfer have been solved by perturbation technique with δ, the slope of the wavy walls as a perturbation parameters. The velocity and the temperature have been analyzed for different variations of the governing parameters G, R, D^{-1},α, β, x and t. Also the stress and rate of heat transfer are evaluated numerically for different variations of the parameters.

2. FORMULATION OF THE PROBLEM

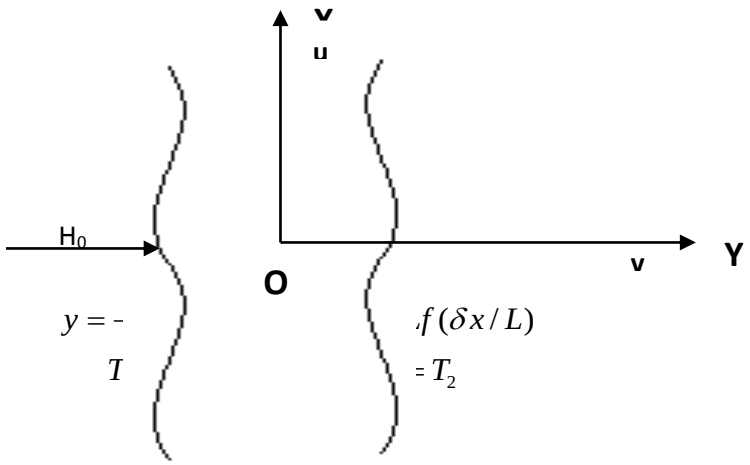

Fig. 1. Schematic diagram of the flow configuration

We consider the unsteady motion of a viscous, electrically conducting, and incompressible fluid through a porous medium in a vertical channel bounded by wavy walls with quadratic density temperature The Boussinesq approximation is used so that the density variation will be considered only in the buoyancy force. A uniform magnetic field of strength Ho is applied transverse to the boundaries. The viscous and Darcy dissipations are neglected in comparison to the flow by conduction and convection. Assuming the magnetic Reynolds number to be small we neglect the induced magnetic field in comparison to the applied field. Also the kinematic viscosity ν, the thermal conductivity k are treated as constants. We choose a rectangular Cartesian system O(x , y) with x-axis in the direction of motion and y-axis in the vertical direction and the walls are taken at y = ± L f(δx/L), where 2L is the distance between the walls, f is a twice differentiable function and δ is a small parameter proportional to the boundary slope. A linear density temperature variation is assumed with ρ_e and Te is the

density and temperature in the equilibrium state. The flow is maintained by an oscillatory volume flux rate for which a characteristic velocity is defined as

$$q(1+e^{i\omega t}) = \left(\frac{1}{L}\right)\int_{-Lf}^{Lf} u\,dy \tag{5.1}$$

The equations governing the unsteady and heat transfer in Cartesian coordinate system O(x, y, z), in the absence of any input electric field are

Equation of continuity

$$\frac{\partial u}{\partial x} + \frac{\partial v}{\partial y} = 0 \tag{5.2}$$

Equation of linear momentum

$$\rho_e\left(\frac{\partial u}{\partial t} + u\frac{\partial u}{\partial x} + v\frac{\partial u}{\partial y}\right) = -\frac{\partial p}{\partial x} + \mu\left(\frac{\partial^2 u}{\partial x^2} + \frac{\partial^2 u}{\partial y^2}\right) - \left(\frac{\sigma\mu_e^2 H_o^2}{\rho_e}\right)u - \left(\frac{\mu}{k}\right)u - \rho g \tag{5.3}$$

$$\rho_e\left(\frac{\partial v}{\partial t} + u\frac{\partial v}{\partial x} + v\frac{\partial v}{\partial y}\right) = -\frac{\partial p}{\partial y} + \mu\left(\frac{\partial^2 v}{\partial x^2} + \frac{\partial^2 v}{\partial y^2}\right) - \left(\frac{\mu}{k}\right)v \tag{5.4}$$

Equation of energy

$$\rho_e C_p\left(\frac{\partial T}{\partial t} + u\frac{\partial T}{\partial x} + v\frac{\partial T}{\partial y}\right) = \lambda\left(\frac{\partial^2 T}{\partial x^2} + \frac{\partial^2 T}{\partial y^2}\right) + Q - \frac{\partial q_r}{\partial y} \tag{5.5}$$

Equation of state

$$\rho - \rho_e = -\beta\rho_e(T - T_e)^2 \tag{5.6}$$

where ρ_e is the density of the fluid in the equilibrium state, Te is the temperature in the equilibrium state. (u, v) are the velocity components along O(x, y) directions, p is the pressure, T is the temperature in the flow region,ρis the density of the fluid, μ is the constant coefficient of viscosity, Cp is the specific heat at constant pressure, λ is the coefficient of thermal conductivity, k is the permeability of the porous medium, β is the coefficient of thermal expansion, σ is the electrical conductivity , μe is the magnetic permeability of the medium, q_r is the radiative heat flux and Q is the strength of the constant internal heat source.

The fluid considered is gray, absorbing-emitting but non-scattering and hence the radiative heat flux term in simplified by using Rosseland approximation (61a) as

$$q_r = -\frac{4\sigma_*}{3\beta_R}\frac{\partial(T'^4)}{\partial y} \tag{5.5a}$$

where q_r represents the radiative heat flux in the y-direction, σ_* is the Stefan-Boltzmann constant and β_R is the mean absorption coefficient. We assume that the temperature difference with in the flow are sufficiently small such that T'^4 may be expressed as a linear

function of the temperature. This is accomplished by expanding T'^4 in a Taylors series about T_e and neglecting higher order terms such that

$$T'^4 \cong 4T_e^3 T - 3T_e^3 \qquad (5.5b)$$

In the equilibrium state

$$0 = -\frac{\partial p_e}{\partial x} - \rho_e g \qquad (5.5c)$$

where $p = p_e + p_D, p_D$ being the hydrodynamic pressure and in this state the temperature gradient balances the heat flux generated by source Q.

The flow being two-dimensional, in order to maintain the compatibility of the equations (5.4) and (5.6) the temperature in the flow field must be a general function of x and y. However temperature over the boundary walls may be kept constant assuming the temperature dependence on the walls to be a function of $\eta = y / f(x)$

The boundary conditions for the velocity and temperature fields are

$u = 0,\ v = 0,\ T = T_1(\eta)$ on $y = -L\ f(\delta x/L)$

$u = 0,\ v = 0,\ T = T_2(\eta)$ on $y = L\ f(\delta x/L)$ (5.7)

In view of the continuity equation we define the stream function ψ as

$$u = \psi_y,\ v = -\psi_x \qquad (5.8)$$

Eliminating pressure p from equations (5.3) & (5.4) and using (5.8) the equations governing the flow in terms of ψ are

$$\left[(\nabla^2\psi)_t + \psi_x(\nabla^2\psi)_y - \psi_y(\nabla^2\psi)_x\right] = \nu\nabla^4\psi + 2\beta g(T - T_0)(T - T_0)_y - \left(\frac{\nu}{k}\right)\nabla^2\psi - \left(\frac{\sigma\mu_e^2 H_o^2}{\rho_e}\right)\frac{\partial^2\psi}{\partial y^2} \qquad (5.9)$$

$$\rho_e C_p\left(\frac{\partial T}{\partial t} + \frac{\partial\psi}{\partial y}\frac{\partial T}{\partial x} - \frac{\partial\psi}{\partial x}\frac{\partial T}{\partial y}\right) = \lambda\nabla^2 T + Q + \frac{16\sigma^{\bullet}T_e^3}{3\beta_R}\frac{\partial^2 T}{\partial y^2} \qquad (5.10)$$

Introducing the non-dimensional variables in (5 .9) & (5.10) as

$$x' = x/L,\ y' = y/L,\ t' = t\varpi,\ \Psi' = \Psi/qL,\ \theta = \frac{T - T_e}{T_2 - T_e} \qquad (5.11)$$

the governing equations in the non-dimensional form (after dropping the dashes) are

$$\gamma\left((\nabla^2\psi)_t + R\frac{\partial(\psi, \nabla^2\psi)}{\partial(x, y)}\right) = \nabla^4\psi + 2\left(\frac{G}{R}\right)\theta\theta_y - D^{-1}\nabla^2\psi - M^2\frac{\partial^2\psi}{\partial y^2} \qquad (5.12)$$

and the energy equation in the non-dimensional form is

$$P_1\gamma^2\frac{\partial\psi}{\partial t} + P_1 R\left(\frac{\partial\psi}{\partial y}\frac{\partial\theta}{\partial x} - \frac{\partial\psi}{\partial x}\frac{\partial\theta}{\partial y}\right) = \nabla^2\theta + \alpha_1 \qquad (5.13)$$

with the corresponding boundary conditions

$$\psi(+1)-\psi(-1)=(1+ke^{i\omega t})$$

$$\frac{\partial\psi}{\partial x}=0,\ \frac{\partial\psi}{\partial y}=0\quad,\theta=\frac{T_1-T_e}{T_2-T_e}=h,say\qquad on\ y=-f(\delta x)$$

$$\frac{\partial\psi}{\partial x}=0,\ \frac{\partial\psi}{\partial y}=0\quad,\theta=1\qquad\qquad on\ y=f(\delta x)$$

$$\frac{\partial\theta}{\partial y}=0,\quad at\quad y=0 \qquad (5.14)$$

where

$R=\frac{qL}{\nu}$ (the Reynolds number)

$G=\frac{\beta g(T_2-T_e)L^3}{\nu^2}$ (the Grashof number)

$\mathrm{P}=\frac{\mu c_p}{k_1}$ (the Prandtl number),

$D^{-1}=\frac{L^2}{k}$ (the Darcy parameter),

$N=\frac{\beta_R\lambda}{4\sigma^{\bullet}T_e^3}$ (the radiation parameter)

$\gamma^2=\frac{\omega L^2}{\nu}$ $(the Wormsely\ Number)$

$M^2=(\frac{\sigma\mu_e^2H_o^2L^2}{\nu^2})$ (the Hartmann number)

$\alpha=\frac{QL^2}{\lambda}$ $(the\ heat\ source\ parameter)$

$P_1=\frac{3NP}{3N+4}$ $\alpha_1=\frac{3N\alpha}{3N+4}$

3. ANALYSIS OF THE FLOW

Introduce the transformation such that

$\bar{x}=\delta x$, $\frac{\partial}{\partial x}=\delta\frac{\partial}{\partial\bar{x}}$

Then

$$\frac{\partial}{\partial x}\sim O(\delta)\ \rightarrow\frac{\partial}{\partial\bar{x}}\sim O(1)$$

For small values of δ<<1 the flow develops slowly with axial gradient of order δ and hence we take $\frac{\partial}{\partial \bar{x}} \sim O(1)$

Using the above transformation the equations (5.12)&(5.13) reduce to

$$\gamma\left((F^2\psi)_t + R\frac{\partial(\psi, F^2\psi)}{\partial(x,y)}\right) = F^4\psi + 2\left(\frac{G}{R}\right)\theta\theta_y - D^{-1}F^2\psi - M^2\frac{\partial^2\psi}{\partial y^2} \quad (5.15)$$

$$P_1\gamma^2\frac{\partial\psi}{\partial t} + \delta P_1 R\left(\frac{\partial\psi}{\partial y}\frac{\partial\theta}{\partial x} - \frac{\partial\psi}{\partial x}\frac{\partial\theta}{\partial y}\right) = F^2\theta + \alpha_1 \quad (5.16)$$

where

$$F^2 = \delta^2\frac{\partial^2}{\partial \bar{x}^2} + \frac{\partial^2}{\partial y^2}$$

The flow develops slowly with axial gradient of order δ and hence we take $\frac{\partial}{\partial \bar{x}} \sim O(1)$.

We may note that the maintenance of slowly varying axial boundary temperature gives rise to the convection currents and in view of the compatibility at the zeroth order level

We adopt the perturbation scheme and write

$$\psi(x,y,t) = (\psi_0 + ke^{it}\bar{\psi}_0) + \delta(\psi_1 + ke^{it}\bar{\psi}_1) + \ldots\ldots\ldots\ldots$$
$$\theta(x,y,t) = (\theta_0 + ke^{it}\bar{\theta}_0) + \delta(\theta_1 + ke^{it}\bar{\theta}_1) + \ldots\ldots\ldots\ldots \quad (5.17)$$

On substituting (5.17) in (5.15) - (5.16) and separating the like powers of δ the equations and respective conditions to the zeroth order on introducing the transformation

$\eta = \frac{y}{f(\bar{x})}$ are

$$\theta_{0,\eta\eta} = -\alpha_1 f^2 \quad (5.18)$$

$$\psi_{0,\eta\eta\eta\eta} - M_1^2 f^2(\psi_{0,\eta\eta}) = -2(\frac{G}{R}f^3)\theta_0\,\theta_{o,\eta} \quad (5.19)$$

$$\bar{\theta}_{0,\eta\eta} - (iP_1\gamma f^2)\bar{\theta}_0 = 0 \quad (5.20)$$

$$\bar{\psi}_{0,\eta\eta\eta\eta} - (D^{-1} + M^2 + i\gamma^2)\bar{\psi}_{0,\eta\eta} = -2(\frac{G}{R}f^3)(\theta_0\bar{\theta}_{0,\eta} + \bar{\theta}_0\,\theta_{0,\eta}) \quad (5.21)$$

$$\theta_0(+1) = 1, \theta_0(-1) = h \quad (5.22)$$

$$\psi_o(+1)-\psi_o(-1)=1,\psi_{0,\eta}(\pm1)=0,\psi_{0,x}(\pm1)=0$$

(5.23)

$$\bar{\theta}_o(\pm1)=0,$$

(5.24)

$$\bar{\psi}_o(+1)-\bar{\psi}_o(-1)=1,\bar{\psi}_{0,\eta}(\pm1)=0,\bar{\psi}_{0,x}(\pm1)=0$$

(5.25)

The equations to the first order are

$$\theta_{1,\eta\eta}=-(P_1Rf^2)(\psi_{0,\eta}\theta_{0,x}-\psi_{0,x}\theta_{0,\eta})$$

(5.26)

$$\psi_{1,\eta\eta\eta\eta}-(M_1^2f^2)\psi_{1,\eta\eta}=-2(\frac{G}{R}f^3)(\theta_1\theta_{0,\eta}+\theta_0\theta_{1,\eta_0})+Rf(\psi_{o,\eta}\psi_{o,x\eta\eta}-\psi_{o,x}\psi_{0,\eta\eta\eta}-(\frac{2f'}{f})\psi_{0,\eta}\psi_{o,\eta\eta})$$

$$\bar{\theta}_{1,\eta\eta}-(iP_1\gamma f^2)\bar{\theta}_1=(P_1Rf^2)(\psi_{0,\eta}\bar{\theta}_{0,x}-\psi_{0,x}\bar{\theta}_{0,\eta}+\bar{\psi}_{0,x}\theta_{o,\eta})$$

(5.27)

$$\bar{\psi}_{1,\eta\eta\eta\eta}-(M_1^2f^2)\bar{\psi}_{1,\eta\eta}=-2(\frac{G}{R}f^3)(\theta_{1,\eta}\theta_0+\theta_{0,\eta}\theta_1)+Rf(\bar{\psi}_{o,\eta}\psi_{o,x\eta\eta}-\psi_{o,x}\bar{\psi}_{0,\eta\eta\eta}+\psi_{o,\eta}\bar{\psi}_{o,x\eta\eta},-\bar{\psi}_{o,x}\psi_{0,\eta\eta\eta})$$

(5.28)

The corresponding boundary conditions are

$$\theta_1(+1)=0,\qquad \theta_1(-1)=0$$

(5.29)

$$\psi_1(+1)-\psi_1(-1)=0,\psi_{1,\eta}(\pm1)=0,\psi_{1,x}(\pm1)=0$$

(5.30)

$$\bar{\theta}_1(\pm1)=0,$$

(5.31)

$$\bar{\psi}_1(+1)-\bar{\psi}_1(-1)=0,\bar{\psi}_{1,\eta}(\pm1)=0,\qquad \bar{\psi}_{1,x}(\pm1)=0$$

(5.32)

Solving the equations (5.18)- (5.28) subject to the relevant boundary conditions we obtain

$$\theta_0=-\frac{\alpha_1f^2}{2}\eta^2+a_1\eta+a_2$$

$$\psi_0=a_{12+}+a_{13}\eta+a_{14}Ch(\beta_1\eta)+a_{15}Sh(\beta_1\eta)$$

$$\bar{\theta}_0=0$$

$$\bar{\psi}_0=a_{16}+a_{17}\eta c+a_{18}Ch(\beta_2\eta_)+a_{19}Sh(\beta_2\eta)$$

$$\theta_1=0.5a_{23}\eta^2+(a_{24}/6)\eta^3+(a_{25}/12)\eta^4+(\frac{a_{26}}{\beta_1^2})Ch(\beta_1\eta)+a_{27}\eta Ch(\beta_1\eta)+a_{28}\eta^2Ch(\beta_1\eta)+a_{30}\eta Sh(\beta_1\eta)$$

$$\psi_1 = B_1 + B_2\eta + B_3 Ch(\beta_1\eta) + B_4 Sh(\beta_1\eta) + \phi_1(\eta)$$

$$\begin{aligned}\phi_1(\eta) &= a_{78}\eta - a_{79}\eta^2 - a_{80}\eta^3 - a_{81}\eta^4 - a_{82}\eta^5 - a_{83}\eta^6 - a_{84}\eta^7 \\ &+ a_{85}\eta\, Ch(\beta_1\eta) + a_{86}\eta Sh(\beta_1\eta) + a_{87}\eta^2 Sh(\beta_1\eta + a_{88}\eta^2 Sh(\beta_1\eta) \\ &+ a_{89} Sh(2\beta_1\eta) + a_{90} Ch(2\beta_1\eta) + a_{93}\eta^3 Sh((\beta_1\eta) + a_{92}\eta^3 Ch((\beta_1\eta)\end{aligned}$$

$$\begin{aligned}\bar{\theta}_1 &= B_{13} + B_{14}\eta + B_{15}\eta^2 + B_{16} Ch(\beta_2\eta) + B_{17} Sh(\beta_2\eta) + B_{118}\eta Ch(\beta_2\eta) \\ &+ B_{19}\eta Sh(\beta_2\eta) + B_{20}\eta^2 Ch(\beta_2\eta)\end{aligned}$$

$$\bar{\psi}_1 = e_1 + e_2\eta + e_3 Ch(\beta_1\eta) + e_4 Sh(\beta_1\eta) + \phi_2(\eta)$$

$$\begin{aligned}\phi_2(\eta) &= B_{75} Sh(\beta_1\eta) - B_{76} Sh(\beta_1\eta) - B_{76} Sh(\beta_5\eta) + B_{79}\eta Ch(\beta_4\eta) + B_{78}\eta Ch(\beta_5\eta) \\ &- B_{79} Sh(\beta_2\eta) - B_{80}\eta Ch(\beta_2\eta) - B_{81}\eta Sh(\beta_1\eta) - B_{82}\eta^2 Sh(\beta_1\eta) + B_{83}\eta Ch(\beta_1\eta) \\ &+ B_{84} Ch(\beta_4\eta) - B_{85} Ch(\beta_5\eta) + B_{86} + B_{87}\eta^3 + B_{88}\mu^4 - B_{89}\eta^2 + B_{90}\eta^5 - B_{91}\eta^3 \\ &- B_{92} Sh(\beta_3\eta)\end{aligned}$$

The shear stress on the channel walls is given by

$$\tau = \frac{\sigma_{xy}(1 - f'^2) + (\sigma_{yy} - \sigma_{xx}) f'^2}{(1 + f'^2)}$$

where

$$\sigma_{ij} = -p\delta_{ij} + 2\mu e_{ij}$$

$$\sigma_{xx} = \frac{\partial u}{\partial x},\ \sigma_{yy} = \frac{\partial v}{\partial y},\ \sigma_{zz} = \frac{\partial w}{\partial z},\ \sigma_{xy} = 0.5\left(\frac{\partial u}{\partial y} + \frac{\partial v}{\partial x}\right)$$

and the corresponding expressions are

$$(\tau)_{\eta=-1} = ((1 - f'^2)(e_{24} + ke^{it}e_2) + \delta((1 - f'^2)(e_9 - (\frac{2f'}{f})(e_3 + ke^{it}e_5)) + O(\delta^2))/(1 + f'^2)$$

$$(\tau)_{\eta=+1} = ((1 - f'^2)(e_1 + ke^{it}e_2) + \delta((1 - f'^2)(e_8 + -(\frac{2f'}{f})(e_3 + ke^{it}e_4) + O(\delta^2))/(1 + f'^2)$$

The local rate of heat transfer coefficient(Nusselt number Nu) on the walls has been calculated using the formula

$$Nu = \frac{1}{\theta_m - \theta_w}\left(\frac{\partial\theta}{\partial y}\right)_{\eta=\pm1}$$

where

$$\theta_m = 0.5\int_{-1}^{1} \theta\, dy$$

and the corresponding expressions are

$$(Nu)_{\eta=+1} = \frac{(e_{10} + \delta(e_{14} + ke^{it}e_{18})}{f(e_{23} - 1)}$$

$$(Nu)_{\eta=-1} = \frac{(e_{11} + \delta(e_{15} + ke^{it}e_{19})}{f(e_{23} - am1)}$$

where $e, e_2, \ldots\ldots\ldots\ldots\ldots, e_{23}, \ldots e_{50}$ are constants given in the appendix.

4. DISCUSSION OF THE NUMERICAL RESULT

The primary aim of our analysis is to investigate the behaviour of temperature induced buoyancy flows taking into account the effect of surface geometry and wall temperature ratio and radiation effect. The flow phenomenon is discussed for different sets of the parameters $G, R, M, \beta, \alpha, N$ *and* γ governing the flow. It should be noted that the flow is basically asymmetric because of distinct surface temperature. For computational purpose we assume that the boundaries to be y= $\pm f\left(\bar{x}\right) = \pm\left(1+\beta e^{-x^2}\right)$ and β >0 correspond to dilated channel and β <0 correspond to a constricted channel. In this analysis we confine our attention to the case β <0. The transformation $\eta = y / f\left(\bar{x}\right)$ reduces the boundaries to $\eta = \pm 1$.

The primary velocity (u) is negative for all |G|. The primary velocity u attains its maximum on the mid-plane. In the heating case u experiences a depreciation with an increase in G>0 and enhances in the cooling case in the entire fluid region (fig 1). Figs.2&3 represents the variation of u with M and R. It is found that for M=2&6, u is negative everywhere in the region thereby indicating a reversal flow in the fluid region. |u| depreciate with increase in M. Thus higher the Lorentz force larger the magnitude of u in the flow region. The variation of u with R shows that u enhances with R in the entire fluid region. The influence of the surface geometry on u is shown in fig.4. For β =-0.3 we notice a reversal flow in the entire region and it disappears for higher $|\beta|$. Higher the constriction of the channel walls smaller |u| in the fluid region. An increase in the wormsely number γ there is an enhancement in u in the fluid region.

The variation of u with heat source parameter α shows that u experiences an enhancement with increase in the strength of the heat source/sink, while an increase in the strength of the heat source/sink depreciates u for $|\alpha| \geq 6$ and for higher $|\alpha|$=6, u enhances remarkably in the entire fluid region (fig 5). The effect of radiation parameter N on u is shown in fig.6. We notice a reversal flow for higher value of the radiation parameter N. An increase in N depreciates the magnitude of u everywhere in the region. we find a depreciation in u and for higher $N \geq 10$, |u| enhances remarkably in the flow region. The variation of u with axial

distance x is shown in the fig. 7. It is found that u enhances marginally with increase in $x \leq \pi$ and reduces with $x \geq 2\pi$ (fig 7).

The secondary velocity v which arises due to the non-uniformity in the boundary is exhibited in fig.8 – 14. It is found that for all parameters v is continuously positive for G>0 and negative for G<0. We found that v experiences an deprecation with increase in G>0 and enhances with G<0. Figs 9 &10 represent a variation of v with R and M. It found that for $M \leq 4$, u enhances in the flow region, while for higher $M \geq 10$, we notice depreciation in v in the entire fluid region. An increase in $R \leq 70$ leads to an enhancement in v depreciates with R ≥ 140. Fig 11 shows the variation of v with β. We found that v continuously positive in the fluid region for different values of $|\beta|$. Larger the constriction smaller v through out the fluid region and for higher constriction for larger v. Fig-12 represents the variation of v with α. It is found that v enhances in the entire fluid region with increase in $|\alpha|$ <0>. An increase in γ reduces v in the left region and enhances it in the right region. Fig.13 represents the variation of v with radiation parameter N. It is found that for $N \leq 1.5$ the secondary velocity v experiences a enhancement in |v| and depreciates with N=5 and it again enhances every where in the region for higher N . Moving along the axial distance |v| enhances with $x \leq \pi$ and depreciates with higher $x \geq 2\pi$ (fig 14).

The non-dimensional temperature (θ) is shown in figs 15 -21 for different parametric values. We follow the convention that the temperature is positive or negative according as the actual temperature is greater or lesser than the equilibrium temperature. It is found that for all |G| the temperature θ is positive. It is found that the actual temperature experiences depreciation in the heating case, and enhances in the cooling case (fig 15). Figs-16&17 represents the variation of θ with M and R. We find that the actual temperature depreciates with M. Also the actual temperature enhances with increase in R. The influence of the surface geometry β on θ is shown in fig 18 it is found that higher the construction of the channel wall larger the actual temperature. The variation of θ with γ reveals on increasing tendency in the actual temperature(fig 16). From fig 19 we notice that θ is positive for $\alpha \leq 4$ and negative for $\alpha \geq 6$ except in the vicinity of $\eta = \pm 1$. The temperature reduces with $\alpha \leq 4$ and enhances with $\alpha \geq 6$.while it enhances with increase in $|\alpha|$(<0). The actual temperature reduces with increase in the radiation parameter $N \leq 4$ and enhances with $N \geq 10$ (fig 20). The variation of θ with time t shows that the actual temperature enhances with increase in x in the left half and enhance in the right half. Moving along the axial direction the actual temperature reduces in the left half and enhances in the right half of the channel with increase in x (fig. 21).

The shear stresses at the boundaries $\eta = \pm 1$ have been evaluated for different values of G, R, $D^{-1}, \alpha, \beta,$ M and $x + \gamma t$ and are represented in the tables 1—8. It is found that the stress at $\eta = 1$ increases in magnitude with increase in G>0 and decreases with G<0 for $D^{-1} \leq 3 \times 10^2$ and enhances for higher $D^{-1} \geq 5 \times 10^2$ while at $\eta = -1$, it decreases with G>0 for $D^{-1} \leq 3 \times 10^2$ and enhances for $D^{-1} \geq 5 \times 10^2$ while it experiences an enhancement with G<0. The pressure / higher larger $|\tau|$ at $\eta = \pm 1$. An increase in the strength of the heat source/sink results in an enhancement in $|\tau|$ at both the walls. The influence of the surface geometry on τ is shown in tables 3&7. It is found that higher the constriction of the channel walls smaller the magnitude τ at $\eta = \pm 1$. An increase in the thermal wave velocity γ reduces $|\tau|$ at $\eta = 1$ and enhances at $\eta = -1$ tables (3&7). The variation of τ with horizontal distance x shows that $|\tau|$ at $\eta = 1$ depreciates with $x \leq \pi/2$ and enhances with higher $x \geq \pi$ with at $\eta = -1$

The average Nusselt number Nu which measure the rate of heat transfer across the boundaries are represent in the table 9 – 12 for different values of G, R, D^{-1}, α, β, M and x. It is found that the rate of heat transfer at $\eta = -1$ increases with increase in |G| (≤ 0) while at $\eta = 1$, |Nu| enhances with G>0 and reduces with G<0 at $D^{-1} \leq 3 \times 10^2$ and enhances for higher $D^{-1} \geq 5 \times 10^2$. The variation of η with D^{-1} and M shows that lesser the permeability of porous medium higher the Lorentz force smaller the magnitude of Nu. The variation of Nu with heat source parameter α reveals that an increase in the strength of heat source/sink enhances |Nu|. The influence of the surface geometry on the rate of heat transfer is shown in tables 11&15. It is found that higher the construction of the channel walls smaller the rate heat transfer at both the walls. An increase in the thermal wave velocity γ results in an enhancement in |Nu| at $\eta = \pm 1$. The behavior of Nu with horizontal distance x shows that an increase $x \leq \pi$ enhances |Nu| for G>0 and reduces it for G<0 while at $x \geq 2\pi$ at both the walls.

REFERENCES

1	Alagoa K.D, Tay. G and Abbey. T.M,	Radiative and free convection effects of a MHD flow through porous medium between infinite parallel plates with time dependent suction, Astrophysics space, Sci, Vol. 260, pp. 455-468,	1999
2	Ayani. M.B and	The effect of radiation on the natural	2006

	Esfahani, J.A,	convection induced by a line heat source. Int. J. Number Method, Heat fluid (UK), 16, p. 28-45,	
3	Bestman. A.R and Adjepong. S.K,	Unsteady hydro magnetic free convection flow with radiative transfer in a rotating fluid, Astrophysics. Space. Sci. V. 143, pp. 73-80,	1998
4	Bharathi,M	Hydrodynamic Mixed Convective Heat Transfer through a porous medium in channels/pipes with Radiation effect,	2009
5	El.Hakeem,M.A	MHD oscillatory flow of free convection radiation through a porous medium with constant suction velocity. Magn.Magn.Mater.,V.220.pp.271-276	2000
6	Eswariah Setty,S	Transient hydro magnetic convection flow through wavy channel, Ph.D. Thesis SKU, Anantapur,	1996
7	Nanda, R.S. and Sharma, V.P,	J. Fluid Mech. 15, p. 419,	1963
8	Gayatri,P	Buoyancy induced hydro magnetic convective Heat Transfer through a porous medium in a channel/pipes with Radiation effect and Heat Source Ph.D. Thesis, SKU, Anantapur,	2009
9	Jaffarunnisa,S	Unsteady hydro magnetic mixed convective flow in a vertical channel with Traveling Thermal wave and Quadratic Temperature Variation,	2009
10	Kumar, A, Singh, N.P. Singh A.K. Kurmar, Atul,	MHD free convection flow of a viscous fluid past a porous vertical plate through a non-homogeneous porous medium with radiation and temperature gradient dependent heat source in a slip flow regime, Ultra Sci, Phy, Sci (India), 18 p. 39-46,	2006
11	Makinde, O.D,	Free convection flow with thermal radiation and Mass Transfer Past a moving vertical porous plate. Int. Common. Heat Mass Transfer (UK) 32 ; 1411- 19,	2005
12	Nanda,R.S and Sharma,V.P	J.Fluid Mech,V.15,p.419	1963
13	Nanda R.S. and Sharma, V.P,	AIAA. J, 1, p. 937,	1963
14	Purushothama Reddy,Y	Unsteady mixed convection flows through vertical channel with varying Gap. Ph.D Thesis, SKU, Anantapur,	1995
15	Ramana Murthy,	Proc. Maths. Soc, B.H.U.V. pp.53- 55	1995

	T.V.and Soundalgekar V.M.		
16	Raptis, A,	Radiation and free convection flow through a porous medium Int. Common. Heat and Mass Transfer 25, 289-295,	1998
17	Ravindra Nath, P	Buoyancy induced hydro magnetic flows through a porous medium Dissipative effects. Ph.D.Thesis, SKU, Anantapur,	2006
18	Soundelgekar,V.M and Pop,I	Int.J.Heat and Mass transfer,V.17,pp.85-90	1974
19	SreeramaChandra Murthy,A	Buoyancy induced hydro magnetic flows through a porous medium-A study, Ph.D thesis, S.K.University, Anantapur, India	1992
20	Taneeja,Rajeev and Jain,N.C	Effect of magnetic field on free convection mass transfer through a porous medium with radiation and variable permeability in slip flow regime, Jnanabha,31/32.p.69	2002
21	Sree Ramachandra Murthy. A,	Ph.D. Thesis, Sri Krishna devaraya University, Anantapur,	1992
22	Kellechar, M.D. and Yang, K.T,	ZAMP, 19, p. 31,	1968
23	A.SreeRamachandra Murthy,	Buoyancy induced hydro magnetic flows through a porous medium – A study. Ph.D. Thesis, SKU, Anantapur,	1992
24	Makinde, O.D,	Free convection flow with thermal radiation and Mass Transfer Past a moving vertical porous plate. Int. Common. Heat Mass Transfer (UK) 32 ; 1411-19,	2005
25	Taneja, Rajeev and Jain, N.C,	Effect of magnetic field on free convection mass transfer flow through porous medium with radiation and variable permeability in slip flow regime, Janabha, 31/32, 69,	2002
26	Soundalgekar, V.M and Pop. I,	Int. J. Heat Mass Transfer V. 17. pp.85-90,	1974

PUNE RESEARCH TIMES
AN INTERNATIONAL JOURNAL OF CONTEMPORARY STUDIES
ISSN 2456-0960
VOL 2, ISSUE 2

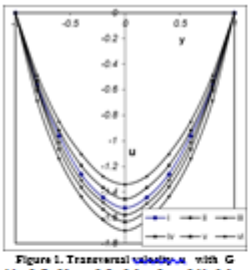

Figure 1. Transversal velocity u with G

$M = 2, R=25, \alpha = 2, \beta=0.5, y =0, m=2, N=0.5, \tau = \pi/$

G	i	ii	iii	iv	v	vi
	10^5	2×10^5	5×10^5	-10^5	-2×10^5	-5×10^5

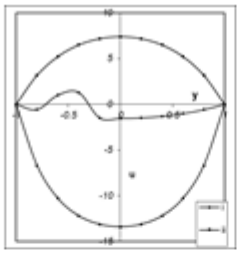

Figure 3. u with M

$G=10^5$, $R=25, \alpha = 2, \beta=0.5, y =0, m=2, N=0.5, \tau = \pi/6$

M	i	ii	iii
	2	4	6

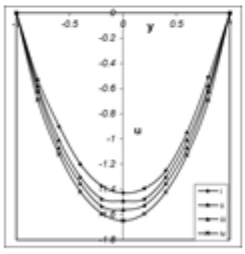

Figure 2. u with R & y

$G=10^5, M = 2, \alpha = 2, \beta=0.5, m=2, N=0.5, \tau = \pi/6$

R	i	ii	iii	iv
y	25	70	140	25
	2	2	2	4

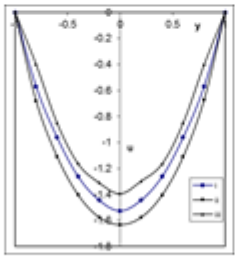

Figure 4. u with β

$G=10^5, M = 2, R=25, \alpha = 2, y =2, m=2, N=0.5, \tau = \pi/6$

β	i	ii	iii
	-0.3	-0.50	-0.70

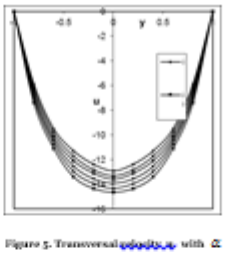

Figure 5. Transversal velocity u with α

$G=10^5, M = 2, R=25, \beta=0.5, y=2, m=2, N=0.5, \tau = \pi$

α	i	ii	iii	iv	v	vi
	2	4	6	-2	-4	-6

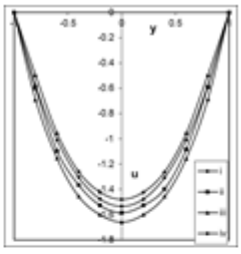

Figure 7. Transversal velocity u

$G=10^5, M = 2, R=25, \alpha = 2, \beta=0.5, y =0, m=2, N=0.5$

τ	i	ii	iii	iv
	$\pi/6$	$\pi/2$	π	2π

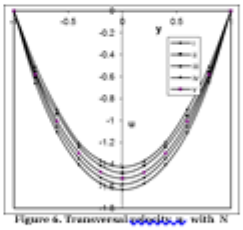

Figure 6. Transversal velocity u with N

$G=10^5, M = 2, R=25, \alpha = 2, \beta=0.5, y =2, m=2, \tau = \pi$

N	i	ii	iii	iv	v
	0.50	1.50	5.00	10.00	100.00

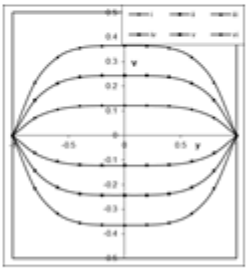

Figure 8. Axial velocity v with G

$M = 2, R=25, \alpha = 2, \beta=0.5, y =0, m=2, N=0.5, \tau = \pi/6$

G	i	ii	iii	iv	v	vi
	10^5	2×10^5	5×10^5	-10^5	-2×10^5	-5×10^5

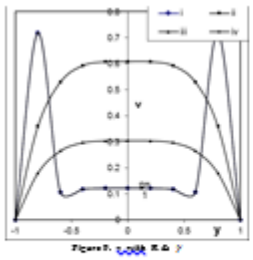

Figure 9. v with R & y

$G=10^5, M = 2, \alpha = 2, \beta=0.5, m=2, N=0.5, \tau = \pi/6$

R	i	ii	iii	iv
y	25	70	140	25
	2	2	2	4

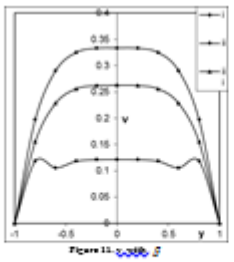

Figure 11. v with β

$G=10^5, M = 2, R=25, \alpha = 2, y =2, m=2, N=0.5, \tau = \pi/6$

β	i	ii	iii
	-0.30	-0.50	-0.70

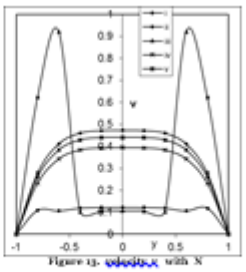

Figure 13. velocity v with N

$G=2, M = 2, R=25, \alpha = 2, \beta=0.5, y =2, m=2, \tau = \pi/6$

N	i	ii	iii	iv	v
	0.50	1.50	5.00	10.00	100.00

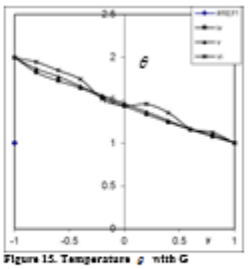

Figure 15. Temperature θ with G

$M = 2, R=25, \alpha = 2, \beta=0.5, y =0, m=2, N=0.5, \tau = \pi/6$

G	i	ii	iii	iv	v	vi
	10^5	2×10^5	5×10^5	-10^5	-2×10^5	-5×10^5

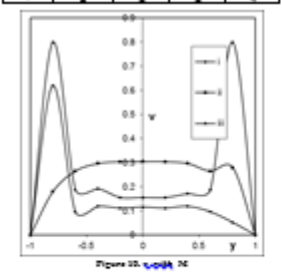

Figure 10. v with M

$G=10^5, R=25, \alpha = 2, \beta=0.5, y =0, m=2, N=0.5, \tau = \pi$

M	i	ii	iii
	2	4	6

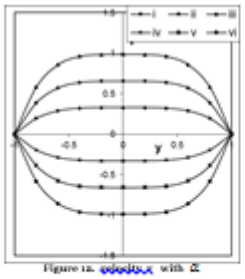

Figure 12. velocity v with α

$G=10^5, M = 2, R=25, \beta=0.5, y =2, m=2, N=0.5, \tau = \pi/6$

α	i	ii	iii	iv	v	vi
	2	4	6	-2	-4	-6

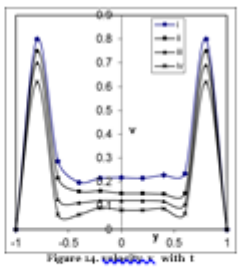

Figure 14. velocity v with τ

$G=2, M = 2, R=25, \alpha = 2, \beta=0.5, y =2, m=2, N=0.5$

τ	i	ii	iii	iv
	$\pi/6$	$\pi/2$	π	2π

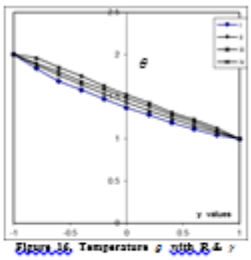

Figure 16. Temperature θ with R & y

$G=2, M = 2, \alpha = 2, \beta=0.5, m=2, N=0.5, \tau = \pi/6$

R	i	ii	iii	iv
y	25	70	140	25
	2	2	2	4

PUNE RESEARCH TIMES
AN INTERNATIONAL JOURNAL OF CONTEMPORARY STUDIES
ISSN 2456-0960
VOL 2, ISSUE 2

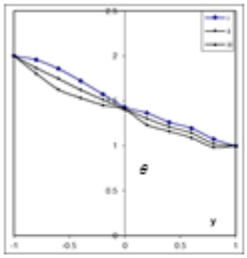

Figure 17. Temperature θ with M

$G=10^5$, $R=65$, $\alpha=2$, $\beta=-0.5$, $y=0$, $m=2$, $N=0.5$, $t=\pi$

	i	ii	iii
M	2	4	6

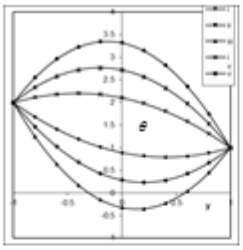

Figure 19. Temperature θ with α

$G=10^5$, $M=2$, $R=65$, $\beta=-0.5$, $y=0$, $m=2$, $N=0.5$, $t=\pi/4$

	i	ii	iii	iv	v	vi
α	2	4	6	-2	-4	-6

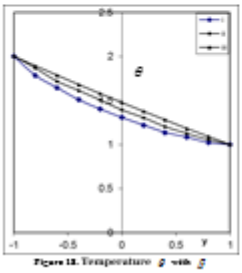

Figure 18. Temperature θ with β

$G=10^5$, $M=2$, $R=65$, $\alpha=2$, $y=0$, $m=2$, $N=0.5$, $t=\pi$

	i	ii	iii
β	-0.30	-0.50	-0.70

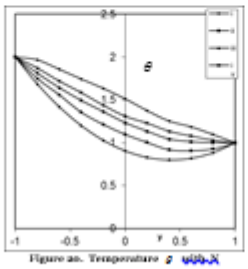

Figure 20. Temperature θ with N

$G=10^5$, $M=2$, $R=65$, $\alpha=2$, $\beta=0.5$, $y=0$, $m=2$, $t=\pi/4$

	i	ii	iii	iv	v
N	0.50	1.50	5.00	10.00	100.00

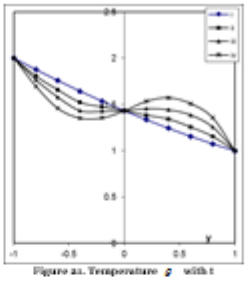

Figure 21. Temperature θ with t

$G=10^5$, $M=2$, $R=65$, $\alpha=2$, $\beta=0.5$, $y=0$, $m=2$, $N=0$.

	i	ii	iii	iv
t	$\pi/4$	$\pi/2$	$\frac{3\pi}{4}$	2π

PUNE RESEARCH TIMES
AN INTERNATIONAL JOURNAL OF CONTEMPORARY STUDIES
ISSN 2456-0960
VOL 2, ISSUE 2

Table :- 1

shear stress $[\tau]_{y=1}$

$m=2, \alpha=2, \beta=-0.5, \gamma=2, x=\pi/4$

G	i	ii	iii	iv	v	vi	vii
10^3	-1.52836	-2.04249	-3.42574	-5.90850	-3.51725	-3.62383	-3.41549
3×10^3	-1.89591	-2.90886	-5.99983	-11.78661	-6.21018	-6.45561	-5.96909
-10^3	-1.04732	-0.82395	0.25441	2.51519	0.83869	0.42666	0.24416
-3×10^3	-0.71747	0.04242	2.82850	8.89380	3.02661	3.25843	2.79776
D^1	10^3	3×10^3	10^3	10^3	10^3	10^3	10^3
M	2	2	2	2	5	10	2
R	35	35	35	35	35	35	70

Table :- 2

shear stress $[\tau]_{y=1}$

$M=2, D^1=10^3, m=2, R=35, \beta=-0.5, \gamma=2, x=\pi/4$

G	i	ii	iii	iv
10^3	-1.52836	-1.6426	-1.8924	-2.5246
3×10^3	-1.89591	-1.9614	-2.1464	-3.2946
-10^3	-1.04732	2.11802	-3.48425	-5.35929
-3×10^3	-0.71747	6.31833	-7.17084	-13.67936
α	2	4	-2	-4

Table :- 3

shear stress $[\tau]_{y=1}$

$M=2, D^1=10^3, m=2, R=35, \alpha=2, x=\pi/4$

G	i	ii	iii	iv
10^3	-5.45120	-3.42574	-1.13672	0.25441
3×10^3	-7.12090	-5.99983	-1.15106	2.82850
-10^3	0.35420	0.25441	-1.12172	0.25441
-3×10^3	3.24120	2.8285	-1.10739	2.82850
β	-0.3	-0.5	-0.7	-0.5
γ	2	2	2	5

Table :- 4

shear stress $[\tau]_{y=1}$

$M=2, D^1=10^3, m=2, R=35, \alpha=2, \beta=-0.5, \gamma=2$

G	i	ii	iii	iv
10^3	-0.82255	0.17783	1.14446	1.14486
3×10^3	-0.97982	1.38645	2.62109	2.62149
-10^3	-0.65699	0.17783	1.14446	1.14486
-3×10^3	-0.49971	1.38645	2.62109	2.62149
x	$\pi/4$	$\pi/2$	π	2π

Table :- 5

shear stress $[\tau]_{y=1}$

$m=2, \alpha=2, \beta=-0.5, \gamma=2, x=\pi/4$

G	i	ii	iii	iv	v	vi	vii
10^3	1.16500	0.91550	-0.17987	-2.44627	-0.25910	-0.35256	-0.20117
3×10^3	0.92696	-0.09470	-3.59808	-10.43129	-3.84309	-4.12950	-3.66350
-10^3	1.34374	1.95047	3.35043	5.83940	3.4424	3.54947	3.37223
-3×10^3	1.50978	2.96067	6.76914	13.82443	7.02639	7.32642	6.83456
D^1	10^3	3×10^3	10^3	10^3	10^3	10^3	10^3
M	2	2	2	2	5	10	2
R	35	35	35	35	35	35	70

Table :- 6

shear stress $[\tau]_{y=1}$

$M=2, D^1=10^3, m=2, R=35, \beta=-0.5, \gamma=2, x=\pi/4$

G	i	ii	iii	iv
10^3	-0.17987	-0.2542	-1.0246	-1.6566
3×10^3	-3.59808	-3.9542	-2.1246	-3.6947
-10^3	3.35043	5.15335	-0.27834	-2.10418
-3×10^3	6.76914	13.06181	-2.90003	-6.27653
α	2	4	-2	-4

Table :- 7

shear stress $[\tau]_{y=1}$

$M=2, D^1=10^3, m=2, R=35, \alpha=2, x=\pi/4$

G	i	ii	iii	iv
10^3	-2.15920	-1.17987	1.14816	3.35043
3×10^3	-4.69890	-3.59808	1.17284	6.76914
-10^3	4.01250	3.3632	1.11378	3.65043
-3×10^3	7.52420	6.7982	1.08410	6.96914
β	-0.3	-0.5	-0.7	-0.5
γ	2	2	2	5

Table :- 8

shear stress $[\tau]_{y=1}$

$M=2, D^1=10^3, m=2, R=35, \alpha=2, \beta=-0.5, \gamma=2$

G	i	ii	iii	iv
10^3	0.73034	2.28177	3.28923	3.28960
3×10^3	0.71773	5.33444	9.27369	9.27531
-10^3	0.74769	2.28177	3.28923	3.28960
-3×10^3	0.76030	5.33444	9.27369	9.27531
x	$\pi/4$	$\pi/2$	π	2π

PUNE RESEARCH TIMES
AN INTERNATIONAL JOURNAL OF CONTEMPORARY STUDIES
ISSN 2456-0960
VOL 2, ISSUE 2

Table - 9

Nusselt number $[Nu]_{x=\pi}$

$m=2, \alpha=2, \beta=-0.5, \gamma=2, x=\pi/4$

G	i	ii	iii	iv	v	vi	vii
10^3	0.33406	0.38781	0.49877	0.65558	0.50522	0.51265	0.59877
3×10^3	0.45392	0.64446	1.18042	2.12169	1.16801	1.20119	1.14042
-10^3	0.28274	0.18166	0.09985	0.00762	0.09557	0.09072	0.12985
-3×10^3	0.14640	0.01345	-0.17496	-0.85763	-0.18407	-0.19484	-0.19496
D^{-1}	10^3	3×10^3	10^3	10^3	10^3	10^3	10^3
M	2	2	2	2	5	10	2
R	35	35	35	35	35	35	70

Table - 10

Nusselt number $[Nu]_{x=\pi}$

$M=2, D^{-1}=10^3, m=2, R=35, \beta=-0.5, \gamma=2, x=\pi/4$

G	i	ii	iii	iv
10^3	0.49877	0.6524	0.6972	0.7982
3×10^3	1.18042	1.3545	1.5672	1.9242
-10^3	0.09985	0.74000	0.14950	0.17336
-3×10^3	-0.17496	-0.39932	0.54653	1.18232
α	2	4	-2	-4

Table - 11

Nusselt number $[Nu]_{x=\pi}$

$M=2, D^{-1}=10^3, m=2, R=35, \alpha=2, x=\pi/4$

G	i	ii	iii	iv
10^3	-1.92488	0.49877	0.17726	0.09985
3×10^3	-1.74631	1.18042	0.17852	-0.17496
-10^3	-1.45881	0.09985	0.17599	0.09985
-3×10^3	-1.59257	-0.17496	0.17473	-0.17496
β	-0.3	-0.5	-0.7	-0.5
γ	2	2	2	5

Table - 12

Nusselt number $[Nu]_{x=\pi}$

$M=2, D^{-1}=10^3, m=2, R=35, \alpha=2, \beta=-0.5, \gamma=2$

G	i	ii	iii	iv
10^3	0.53266	0.34881	0.14818	0.14810
3×10^3	0.64849	-0.45118	-0.58823	-0.58819
-10^3	0.47873	0.34881	0.14818	0.14810
-3×10^3	0.38176	-0.45118	-0.58823	-0.58819
x	0.78560	1.57140	3.24140	6.48280

Table - 13

Nusselt number $[Nu]_{x=\pi}$

$m=2, \alpha=2, \beta=-0.5, \gamma=2, x=\pi/4$

G	i	ii	iii	iv	v	vi	vii
10^3	-0.08660	-0.07162	-0.14359	-0.41930	-0.14771	-0.15243	-0.14359
3×10^3	-0.11484	-0.23506	-0.52045	-1.02267	-0.53858	-0.55966	-0.52045
-10^3	0.03119	0.06595	0.12249	0.18749	0.12547	0.12886	0.12249
-3×10^3	0.09019	0.18335	0.32037	0.45917	0.32715	0.33481	0.32037
D^{-1}	10^3	3×10^3	10^3	10^3	10^3	10^3	10^3
M	2	2	2	2	5	10	2
R	35	35	35	35	35	35	70

Table - 14

Nusselt number $[Nu]_{x=\pi}$

$M=2, D^{-1}=10^3, m=2, R=35, \beta=-0.5, \gamma=2, x=\pi/4$

G	i	ii	iii	iv
10^3	-0.14359	-0.24589	-0.12149	-0.13542
3×10^3	-0.52045	-0.6505	-0.4535	-0.4898
-10^3	0.12249	0.14546	0.07799	0.05643
-3×10^3	0.32037	0.49394	-0.18903	-0.58476
α	2	4	-2	-4

Table - 15

Nusselt number $[Nu]_{x=\pi}$

$M=2, D^{-1}=10^3, m=2, R=35, \alpha=2, x=\pi/4$

G	i	ii	iii	iv
10^3	1.96146	-0.14359	0.06554	0.12249
3×10^3	1.75517	-0.52045	0.06467	0.32037
-10^3	1.44518	0.12249	0.06642	0.12249
-3×10^3	1.58616	0.32037	0.06729	0.32037
β	-0.3	-0.5	-0.7	-0.5
γ	2	2	2	5

Table - 16

Nusselt number $[Nu]_{x=\pi}$

$M=2, D^{-1}=10^3, m=2, R=35, \alpha=2, \beta=-0.5, \gamma=2$

G	i	ii	iii	iv
10^3	-0.15940	-0.01896	0.10918	0.10923
3×10^3	-0.24090	0.55676	0.64771	0.64767
-10^3	-0.11896	0.01896	0.10918	0.10923
-3×10^3	-0.04299	0.55676	0.64771	0.64767
x	0.78560	1.57140	3.24140	6.48280